EAI Endorsed Transactions
on Energy Web
Research Article EAI.EU

Identification and operational optimization of virtual energy storage characteristics for customer-side resources

Shiwang Yang[1,*], Jian Huang[1], Junshi Chen[1], Penghao Sun[1], Ziyi Zhan[1] and Xinyi Zhao[1]

[1]State Grid Zhejiang Lishui Power Supply Company, Lishui, China, 323000

Abstract

INTRODUCTION: This paper addresses the challenges of integrating diverse customer-side resources into virtual energy storage (VES) systems to enhance power system flexibility and renewable energy utilization.
OBJECTIVES: The study aims to develop an integrated framework for the identification and optimal scheduling of VES systems, aggregating multi-type resources such as thermostatically controlled loads, electric vehicles, and distributed energy storage systems.
METHODS: Quantitative models were established to characterize the operational features of each resource. A data-driven clustering algorithm was employed to aggregate heterogeneous resources into unified VES units. A bi-level optimization model was formulated to minimize the aggregator's operational cost while incorporating comfort penalty functions to maintain user satisfaction.
RESULTS: Simulations across four scenarios (sunny, cloudy, high load, high EV penetration) demonstrated significant improvements: the peak-to-valley difference was reduced by 21.6%–28.4%, photovoltaic utilization exceeded 98%, and electricity purchase costs decreased by 4.8%–7.3%.
CONCLUSION: The proposed framework provides an effective and scalable approach for VES scheduling, significantly enhancing renewable energy integration and operational flexibility in modern distributed power systems.

Keywords: Virtual energy storage; Optimal scheduling; Renewable energy integration; Distributed energy resources

Received on 17 November 2025, accepted on 12 December 2025, published on 31 March 2026

doi: 10.4108/ ew.11942

1. Introduction

With the rapid global development of renewable energy, power systems are facing increasingly severe challenges in peak shaving and uncertainty [1-3]. The intermittent and volatile nature of renewable sources such as wind and solar energy leads to instability in power supply, particularly during peak load periods, significantly increasing the pressure on grid dispatch [4,5]. To address this issue, traditional power system dispatch methods are gradually shifting toward demand-side management (DR) and flexible load scheduling [6]. Distributed energy resources on the customer side, such as electric vehicles (EVs), building air conditioning (HVAC) systems, and energy storage systems (ESS), are regarded as potential "virtual energy storage" resources due to their dispatch flexibility and temporal controllability [7-9]. These resources can provide functions similar to physical energy storage without additional hardware investments, thereby enabling grid load balancing and optimized dispatch [10,11].

Scholars both domestically and internationally have conducted extensive research on Virtual Energy Storage

*Corresponding author. Email: 1339230649@qq.com

Systems (VES) [12-15]. Sivaneasan et al. proposed a virtual energy storage capacity estimation method based on demand response management, which assessed the virtual storage potential of residential refrigerators and other devices through simulations and mathematical models. However, their modeling relies on empirical parameters, making it difficult to accurately reflect the diversity of devices and user behaviors [12]. Muessel et al. introduced a deviation modeling-based representation method for electric vehicle virtual energy storage, enabling scalable resource aggregation. Nevertheless, this approach primarily focuses on a single resource type and lacks applicability for the coordinated scheduling of heterogeneous resources [13]. Regarding building air conditioning systems, Jin et al. investigated the virtual energy storage potential of air conditioning loads coupled with buildings, finding that it can effectively reduce operational costs and carbon emissions. However, their study mainly concentrated on a single building type and did not fully account for the diverse needs of different user groups [14]. Additionally, Fu et al. reviewed virtual energy storage modeling methods and pointed out that most existing research focuses on the control and optimization of single resources, with insufficient attention to the comprehensive identification and scheduling strategies for multi-type customer-side resources [15].

In response to the aforementioned research status and existing limitations, this paper proposes an integrated framework for the identification of virtual energy storage characteristics and operational optimization of diverse customer-side resources. First, quantitative models of virtual energy storage characteristics are established for typical customer-side resources such as thermostatically controlled loads, electric vehicles, and energy storage systems, clarifying key parameters such as equivalent capacity, charging/discharging power, and self-discharge rates. Subsequently, a data-driven clustering algorithm is employed to identify and aggregate heterogeneous resources with similar characteristics, forming virtual energy storage units. Finally, a bi-level optimization model is constructed to minimize the total operational cost of aggregators while ensuring user comfort. Simulation case studies verify that the proposed method can effectively identify virtual energy storage potential, achieve coordinated scheduling and economic optimization of multiple resources, and provide theoretical foundations and technical support for the efficient application of virtual energy storage systems.

2. Modeling of Virtual Energy Storage Characteristics for Multi-Type Customer-Side Resources

To accurately characterize the virtual energy storage characteristics of diverse customer-side resources, this paper establishes models for thermostatically controlled loads, electric vehicles, and distributed energy storage systems. Thermostatically controlled loads leverage thermal inertia to adjust power consumption without significantly affecting user comfort, while electric vehicles enable charging and discharging within available time windows. Distributed energy storage systems exhibit well-defined capacity and power constraints. By extracting key parameters such as equivalent capacity, charging/discharging power, self-discharge rate, and temporal flexibility, this approach provides a unified mathematical foundation for subsequent feature identification, clustering analysis, and optimized scheduling, while ensuring user comfort and practical constraint feasibility.

2.1. Virtual Energy Storage Model for Thermostatically Controlled Loads

Thermostatically controlled loads can achieve temporal energy transfer through thermal inertia, thereby exhibiting charging and discharging characteristics analogous to those of energy storage systems. During power system regulation, such loads can modulate their power consumption in response to electricity price fluctuations or changes in system load while maintaining user comfort, thereby fulfilling the role of virtual energy storage [16,17].

Taking air conditioning load as an example, the dynamic behavior of its indoor temperature can be described by a first-order thermal balance model:

$$\frac{dT_{in}}{dt} = \frac{T_{out} - T_{in}}{R \times C} - \frac{P}{COP \times C} \tag{1}$$

Where T_{in} represents the indoor temperature, T_{out} the outdoor temperature, R the building thermal resistance, C the building thermal capacitance, P the cooling power, and COP the coefficient of performance of the air conditioning unit. This equation accounts for both the passive heat exchange due to indoor-outdoor temperature differences and the active cooling regulation provided by the air conditioning system.

Based on the dynamic equations above, the equivalent virtual energy storage parameters of thermostatically controlled loads can be defined as follows:

$$E_{max} = C(T_{max} - T_{min}) \tag{2}$$

$$P_{rate} = P / COP \tag{3}$$

$$k = 1 / R{\cdot}C \tag{4}$$

Where E_{max} denotes the equivalent energy storage capacity of the thermostatically controlled load, representing the amount of thermal energy that can be stored or released within the user-acceptable temperature range; P_{rate} indicates the equivalent charging/discharging power, reflecting the adjustable energy per unit time; k represents the self-discharge rate, characterizing the rate of energy dissipation when the load is inactive; and T_{max} and T_{min} correspond to the upper and lower comfort temperature boundaries, respectively. Through these parameters, the thermostatically controlled load can be abstracted as a virtual energy storage unit with energy constraints, power limitations, and self-discharge characteristics.

Moreover, user comfort serves as a key constraint in the regulation of thermostatically controlled loads. The comfort sensitivity coefficient u_i reflects the extent to which users prioritize indoor comfort over energy cost savings. Its value is typically determined from empirical studies and behavioral surveys, generally ranging from 0.2 to 0.8 [18], where a higher value indicates stricter comfort requirements and a lower value indicates greater flexibility. It can be represented by a utility function:

$$u(T_{in}) = \begin{cases} 1, T_{min} \le T_{in} \le T_{max} \\ \alpha(1-|T_{in}-T_{pref}|/T_{max}-T_{min}), otherwise \end{cases} \quad (5)$$

Where T_{pref} denotes the user's preferred ideal temperature, and α represents the comfort discount coefficient. This utility function quantifies the comfort level of thermostatically controlled loads at different temperatures, and can be incorporated as either a constraint or part of the objective function in optimization scheduling.

In summary, this model not only captures the dynamic response characteristics and virtual energy storage capabilities of thermostatically controlled loads, but also incorporates power constraints, capacity limitations, self-discharge properties, and user comfort considerations, thereby providing a comprehensive mathematical foundation for subsequent aggregation analysis and scheduling optimization.

2.2. Virtual Energy Storage Model for Electric Vehicles

EVs, as flexible demand response resources, can achieve orderly energy temporal shifting by adjusting their charging and discharging schedules in response to electricity price signals. This capability enables peak shaving and valley filling, demonstrating significant VES characteristics [19]. To highlight the VES functionality of EVs, existing studies predominantly develop models from the perspectives of responding to grid price signals and meeting user travel demands [20].

In the model, the daily driving distance and return time of EVs follow a lognormal distribution. The parameters of the lognormal distribution for daily driving distance and return time of EVs are based on regional EV travel survey data. To improve their representativeness at a national level, these parameters are further adjusted using travel behavior statistics from the China Transportation Research Center. This allows the model to realistically reflect the variability in EV usage, including differences in daily travel distances and return times, which is essential for accurately estimating EV availability for vehicle-to-grid (V2G) services within the virtual energy storage framework. While ensuring that the travel needs of vehicle owners are met, the vehicles interact with the grid through time-of-use electricity price incentives.

Using the Monte Carlo simulation method, the return time of each EV $t_f(i)$ can be compared with the end time of off-peak pricing T_{ms} and the start time of peak pricing T_{ns} to determine the optimal start times for charging and discharging. According to the principle of "charging during off-peak hours and discharging during peak hours," the charging periods $T_{chars}(i)$ and discharging periods $T_{dchars}(i)$ for electric vehicle VES can be scheduled as follows:

$$T_{chars}(i) = t_f(i), 0 \le t_f(i) < T_{ms} \quad (6)$$

$$T_{dchars}(i) = \begin{cases} T_{ns}, T_{ms} \le T_f(i) < T_{ns} \\ T_f(i), T_{ns} \le T_f(i) \le 24 \end{cases} \quad (7)$$

The discharge energy $E_{dchar}(i)$ and discharge duration $T_{dchar}(i)$ of electric vehicle VES are determined by the total battery capacity C_{ev}, charging/discharging power P_{ev}, energy consumption per unit distance w, maximum depth of discharge r, SOC limits, and daily driving distance $S(i)$, as expressed in the following formula:

$$E_{dchar}(i) = min\{(SOC_{max} - SOC_{min})C_{ev} - wS(i), rC_{ev}\} \quad (8)$$

$$T_{dchar}(i) = (SOC_{max} - SOC_{min})C_{ev}/P_{ev} - wS(i)/P_{ev} \quad (9)$$

Combining the charging and discharging constraints during peak and off-peak electricity price periods, the discharge end time $T_{dchare}(i)$ and charging end time $T_{chare}(i)$ of electric vehicle VES can be calculated as follows:

$$T_{dchare}(i) = T_{dchars}(i) + T_{dchar}(i) \quad (10)$$

$$T_{chare}(i) = T_{chars}(i) + (\sum_{t=T_{dchare}(i)}^{T_{dchare}(i)} P_{ev} + wS(i))/P_{ev} \quad (11)$$

The charging and discharging electricity of VES at different time periods $E_{ev}(t)$ and the virtual energy state $SOC_{Eev}(t)$ can also be dynamically calculated through corresponding formulas:

$$E_{ev}(t) = \sum_{t=T_1}^{T_2} P_{ev}, \begin{cases} T_1 = T_{chars}, T_2 = T_{chare}, charging \\ T_1 = T_{dchars}, T_2 = T_{dchare}, discharging \end{cases} \quad (12)$$

$$SOV_{E_{ev}}(t+1) = SOV_{E_{ev}}(t) + \eta_{ev}E_{ev}(t)/C_{ev} \quad (13)$$

where η_{ev} is the battery's charging and discharging efficiency.

It should be noted that the virtual energy storage characteristics of electric vehicles are significantly influenced by the behavioral preferences of vehicle owners. Related studies incorporate owners' usage habits to set redundancy constraints for VES indicators and reduce the uncertainty of individual vehicle response behaviors through aggregate control, thereby enhancing the system's robustness and operational stability. Furthermore, some literature proposes methods to increase user participation in VES by setting response willingness, establishing consumer psychological models, and introducing incentive mechanisms. Future research could further integrate various incentive factors into the models to more intuitively reflect the impact of incentive policies on the virtual energy storage characteristic indicators of EVs.

2.3. Virtual Energy Storage Model for Distributed ESS

As an essential component of virtual energy storage, the ESS can realize bidirectional energy regulation through charging and discharging processes, and its operational characteristics can be directly abstracted as a virtual energy storage unit. The modeling mainly considers the energy balance relationship, SOC constraints, charging and discharging power limits, and lifetime degradation factors [21].

During the scheduling period, SOC of the energy storage system changes with the charging and discharging activities, and its dynamic behavior can be expressed by the following equation:

$$SOC_{es}(t+1) = SOC_{es}(t) + \eta_c P_c(t)\Delta t - P_d(t)\Delta t / \eta_d \quad (14)$$

Where $SOC_{es}(t)$ denotes the state of charge of ESS, $P_c(t)$ and $P_d(t)$ represent the charging power and discharging power, respectively, η_c and η_d denote the charging and discharging efficiencies, respectively, Δt is the scheduling time interval.

To ensure the safety and reliability of the energy storage system, the SOC must satisfy the following boundary constraints:

$$SOC_{es,min} \le SOC_{es}(t) \le SOC_{es,max} \quad (15)$$

Here, $SOC_{es,min}$ and $SOC_{es,max}$ are typically determined by the battery characteristics and safety operation requirements, in order to prevent lifespan loss and safety risks caused by deep overcharging or overdischarging.

At the same time, the charging and discharging power is limited by the rated capacity of the device:

$$0 \le P_c(t) \le P_{c,max}, 0 \le P_d(t) \le P_{d,max} \quad (16)$$

On this basis, in order to more accurately reflect the impact of battery lifetime on the scheduling strategy, a degradation cost factor per unit of charged and discharged energy λ_{deg} can be introduced to quantify the battery degradation effect in the optimization objective.

$$C_{deg} = \lambda_{deg}(P_c + P_d)\Delta t \quad (17)$$

Where C_{deg} represents the degradation cost caused by the battery's charging and discharging during the time period. By considering this term in the scheduling optimization model, frequent deep cycles of the energy storage can be effectively avoided, thereby extending the battery's lifespan.

2.4. Unified Modeling and Aggregated Optimization of VES

Feature Identification and Aggregation

In order to unify heterogeneous customer-side resources, their operational characteristics are first represented by a standardized feature vector. For each resource i, the virtual storage capability can be described as:

$$F_i = [E_i, P_{c,i}^{max}, P_{d,i}^{max}, \eta_{c,i}, \eta_{d,i}, \gamma_i, \tau_i, u_i] \quad (18)$$

Where E_i is the equivalent energy capacity, γ_i is the self-dissipation rate, τ_i is the time flexibility index, and u_i reflects user comfort sensitivity.

Clustering K-means algorithms are applied to group similar resources into aggregated VES units. The K-means method is a classical and efficient unsupervised clustering algorithm that partitions heterogeneous customer-side resources into several homogeneous groups by minimizing the distance between samples and their cluster centers. It efficiently handles high-dimensional feature data with low computational complexity and stable convergence, thereby aggregating resources with similar characteristics into unified VES units to provide a concise and accurate representation for subsequent optimization[22]. For the k-th cluster, its equivalent parameters are:

$$E_k = \sum E_i, P_{c,k}^{max} = \sum P_{c,i}^{max}, P_{d,k}^{max} = \sum P_{d,i}^{max} \quad (19)$$

with energy boundaries:

$$S_k^{min} = \sum E_i SOC_i^{min}, S_k^{max} = \sum E_i SOC_i^{max} \quad (20)$$

This aggregation preserves the essential flexibility and capacity of original resources while reducing the dimensionality of the optimization problem.

Aggregated Energy State Dynamics

The temporal dynamics of aggregated energy states are given by:

$$S_k(t+1) = S_k(t) + (\eta_{c,k} P_{c,k}(t) - P_{c,k}(t)/\eta_{d,k})\Delta t - \gamma_k S_k(t)\Delta t \quad (21)$$

where $S_k(t)$ is the SOC of unit k at time t .

The operational limits are:

$$S_k^{min} \le S_k(t) \le S_k^{max}, 0 \le P_{c,k}(t) \le P_{c,k}^{max}, 0 \le P_{d,k}(t) \le P_{d,k}^{max} \quad (22)$$

To enforce mutual exclusiveness of charging/discharging, a binary variable $z_k(t)$ can be introduced:

$$P_{c,k}(t) \le z_k(t) P_{c,k}^{max}, P_{d,k}(t) \le (1 - z_k(t)) P_{d,k}^{max}, z_k(t) \in \{0,1\} \quad (23)$$

Aggregator Optimization Model

At the aggregator level, the objective is to minimize energy procurement cost while accounting for degradation cost and user comfort:

$$J = \sum_{t=1}^{T} c(t) G(t) \Delta t + \sum_{k=1}^{K} \sum_{t=1}^{T} C_{k,deg}(P_{c,k}(t) + P_{d,k}(t))\Delta t + \lambda_{cmf} Discomfort \quad (24)$$

where $c(t)$ is electricity price, $G(t)$ is grid import, $C_{k,deg}$ is degradation coefficient, and λ_{cmf} is comfort penalty factor.

The power balance is expressed as:

$$G(t) + \sum_{k=1}^{K} P_{d,k}(t) = L(t) + \sum_{t=1}^{T} P_{c,k}(t) - P_{PV}(t), \forall t \quad (25)$$

where $L(t)$ is uncontrollable load and $P_{PV}(t)$ is PV generation.

3. Simulation Setup and Scenarios

3.1. Simulation Environment and Parameter Settings

The simulations are conducted in the MATLAB R2023a environment, where the optimization model is formulated as a mixed-integer linear program (MILP) and solved using IBM ILOG CPLEX Optimization Studio (version 22.1). MILP is chosen because it can simultaneously handle binary decision variables and continuous variables. The scheduling horizon is set to a typical day of 24 hours with a time step of Δt= 1hour. This temporal resolution adequately captures the intra-day variations of load, PV generation, and user behavior while keeping the problem size computationally tractable.

The test system considers three types of customer-side resources: TCLs, EVs, and ESSs. TCLs are modeled through indoor temperature dynamics subject to comfort constraints; EVs are characterized by stochastic arrival/departure times and travel-related energy requirements; and ESSs are modeled with SOC dynamics, efficiency, and degradation costs. Representative parameters used in the numerical simulations are summarized in Table 1.

Table 1. Parameter settings of customer-side resources.

Resource	Parameter	Value	Description
TCLs	Rated power	3.5 kW	Device rated capacity
	COP	3.0	Coefficient of performance
	Comfort range	[22, 26] ℃	Indoor temperature bound
	Thermal capacity C	3.0 kWh/ ℃	
	Thermal resistance R	2.0 ℃/kW	
EVs	Battery capacity	60 kWh	Mobile storage size
	Max charge/discharge	7 kW	Per EV
	Charging/discharging efficiency	0.95	
	SOC limits	[0.2, 0.9]	
	Arrival/Departure	18:00-8:00	
ESSs	Capacity	100 kWh	Per unit
	Max charge/discharge	50 kW	Per unit
	Charging/discharging efficiency	0.95	
	SOC limits	[0.1, 0.9]	
	Degradation cost	0.03 yuan/kWh	Linearized cycling cost

A time-of-use (TOU) electricity tariff is adopted to capture the impact of demand-side response in Table 2:

Table 2. The TOU electricity tariff.

Period	Time interval	Price (yuan/kWh)
Off-peak	0:00–7:00	0.30
Flat	8:00–16:00	0.50
Peak	17:00–21:00	0.90
Evening	22:00–23:00	0.40

3.2. Scenario Design

To comprehensively evaluate the applicability and robustness of the proposed VES optimization framework, four representative scenarios are designed in Table 3.

Table 3. Scenario settings.

Scenario	Description	Key Feature
A - Sunny	PV operates at full output with a peak of 145 kW	Renewable abundance
B - Cloudy	PV generation is reduced to 30% of the sunny profile	Renewable scarcity
C - High demand	Baseline load increased by 20%	Load stress
D - High EV	Number of EVs doubled (60 → 120)	Impact of transportation electrification

Scenario A represents a sunny day, where PV output follows a clear-sky curve with a peak of 145 kW at noon, highlighting the synergy between renewable generation and VES. Scenario B corresponds to a cloudy day, where PV generation is reduced to 30% of the sunny profile, simulating renewable scarcity and intermittency. Scenario C represents a high-demand condition, where the baseline load is uniformly increased by 20% across all time slots, reflecting grid stress during peak seasons or extreme weather. Scenario D corresponds to high EV penetration, where the EV fleet is doubled from 60 to 120 units, examining the impact of transportation electrification on system flexibility and scheduling performance.

Each scenario is simulated for 24 hours under the same modeling framework. The outputs include grid power exchange, charging/discharging strategies of VES units, comfort indicators, EV departure SOC satisfaction, and total system operating cost. By comparing across scenarios, the peak-shaving capability and economic benefits of VES

under diverse operating conditions can be systematically assessed.

4. Simulation Results and Analysis

Based on the previously established models and scenario designs, this section presents 24-hour optimal scheduling simulations for four typical days (sunny, cloudy, high load, and high EV penetration). The simulations systematically analyze the performance of VES in peak shaving and valley filling, self-consumption of PV generation, and economic operation. The simulation results include user load, PV output, VES charging and discharging power, SOC, system load, and grid electricity purchase/cost indicators, providing quantitative evidence for evaluating the performance of VES optimal scheduling strategies.

4.1. Typical Daily Energy Profiles and Mismatch Characteristics

Under sunny conditions (see Fig. 1(A)), the PV output exhibits a clear single-peak solar irradiance pattern. PV power gradually rises from 7:00 in the morning, reaching its peak between 10:00 and 13:00, with a maximum of about 145 kW at 12:00. The total daily generation is approximately 1,100 kWh, of which the single-peak period (10:00–13:00) contributes around 42%. The user load shows a typical double-peak pattern in the morning and evening, with the morning peak occurring between 7:00 and 9:00 at about 115–120 kW and the evening peak between 18:00 and 21:00 at around 120 kW. Between 11:00 and 14:00, PV output significantly exceeds the load, resulting in surplus energy of about 48 kWh. Without energy storage, this surplus would lead to PV curtailment.

Under cloudy conditions (see Fig. 1(B)), the PV peak drops sharply to around 45 kW, and the total daily PV generation is only 30–35% of that on a sunny day. The midday surplus nearly disappears, while the evening load deficit still exists. The user load curve shows no significant change, indicating an increased reliance on the grid during cloudy days. In this case, the system's demand for peak-shaving resources (such as VES) is significantly increased to ensure effective support for the evening peak load while maximizing the utilization of the limited PV generation.

Under high-load conditions (see Fig. 1(C)), the baseline load increases by 20%, resulting in a midday peak of approximately 138 kW and an evening peak of about 144 kW. Although PV generation still follows the sunny-day pattern, the increased load exacerbates the mismatch between PV output and load. While some PV surplus remains at noon, the evening load deficit widens, requiring the energy storage system to provide higher discharge power during the night peak to reduce dependence on high-cost grid electricity.

Under high EV penetration (see Fig. 1(D)), the number of electric vehicles on the customer side increases to 120, significantly raising the evening charging load and pushing the evening peak to about 155 kW. Meanwhile, the increased nighttime off-peak charging demand provides more scheduling flexibility for VES. In this scenario, VES needs not only to absorb midday PV surplus but also to meet nighttime EV charging demand, ensuring the system's peak-valley load regulation capability for the following day.

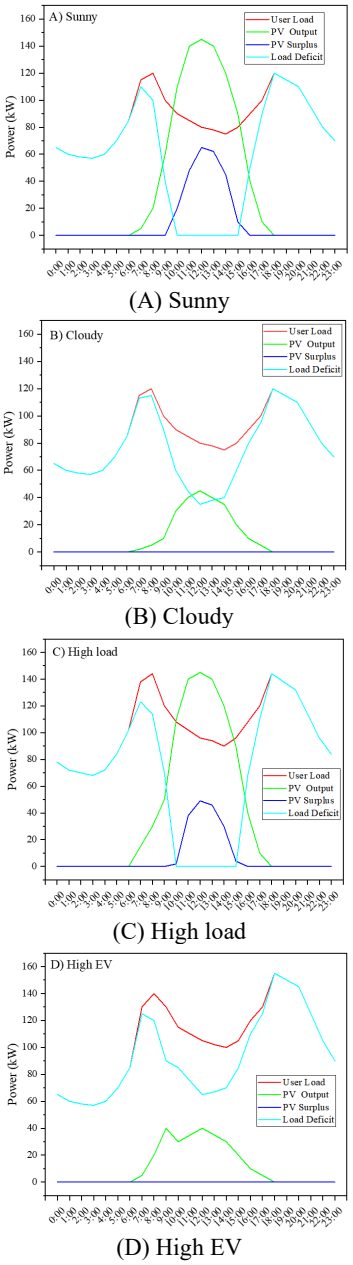

(A) Sunny

(B) Cloudy

(C) High load

(D) High EV

Figure 1. Typical Daily Energy Profiles for the Four Scenarios

By comparing the four scenarios, a consistent temporal pattern of "relatively abundant PV at noon—high load in the evening" can be observed. This pattern reveals two key

issues: (1) underutilized midday PV surplus: during sunny and high-load conditions, PV output exceeds load demand at noon, leading to potential PV curtailment. Without energy storage, the surplus cannot be converted into economic value; (2) high evening peak pressure: especially under cloudy, high-load, or high EV penetration conditions, the mismatch between evening peak load and PV generation increases, resulting in higher grid electricity dependence, elevated peak electricity costs, and increased grid operational stress.

Overall analysis indicates that under optimal VES scheduling, by absorbing surplus PV energy at noon, discharging in the evening, and replenishing during nighttime off-peak periods, the system can effectively mitigate PV-load temporal mismatches, enhance PV self-consumption, and reduce grid electricity costs.

4.2. Virtual Energy Storage Dispatch Behavior Analysis

To mitigate the temporal mismatch between PV output and user load, the system incorporates VES and employs optimized scheduling to achieve intra-day energy shifting. The simulation results indicate that VES exhibits a typical dynamic pattern of "midday charging - evening discharging - nighttime replenishment" with its charging and discharging behavior closely aligned with PV generation and load demand (see Fig. 2).

During the daytime PV peak period (10:00–14:00), when PV generation exceeds load demand, VES primarily operates in the charging mode. In Scenario A, VES charging power remains within 28–40 kW, and SOC rises from 62% to 70%, effectively absorbing about 48 kWh of surplus midday PV energy and significantly reducing curtailment. In Scenario B, PV output declines to a peak of approximately 45 kW, and VES charging power decreases to 15–20 kW, with SOC rising only from 56% to 62% at midday. Although the available energy is limited, VES still ensures the effective utilization of scarce PV generation. In Scenario C, corresponding to high load conditions, the mismatch between PV output and load intensifies. VES charging power ranges from 25–45 kW, and SOC increases to around 72%, partially alleviating the power deficit. In Scenario D, under high EV penetration, VES maintains SOC within the range of 70–78% during midday, balancing the need for evening discharging and nighttime replenishment.

During the evening peak period (18:00–21:00), when PV output is nearly zero, VES switches to discharging mode to relieve system stress. In Scenario A, discharging power reaches 30–40 kW, and SOC decreases from 50% to 35–38%, significantly reducing peak-hour grid purchases. In Scenario B, due to insufficient midday charging, discharging power is limited to 25–35 kW, with SOC dropping to 30–32%, still providing some peak-shaving effect. In Scenario C, the evening power deficit further enlarges, and VES discharging power increases to 40–50 kW, with SOC declining from 48% to 32%, ensuring stable power supply under high-load conditions. In Scenario D, large-scale EV charging exacerbates evening demand, with VES discharging power maintained at 35–45 kW, and SOC dropping from 48% to 32%, demonstrating its flexible regulation capability under multiple load stresses.

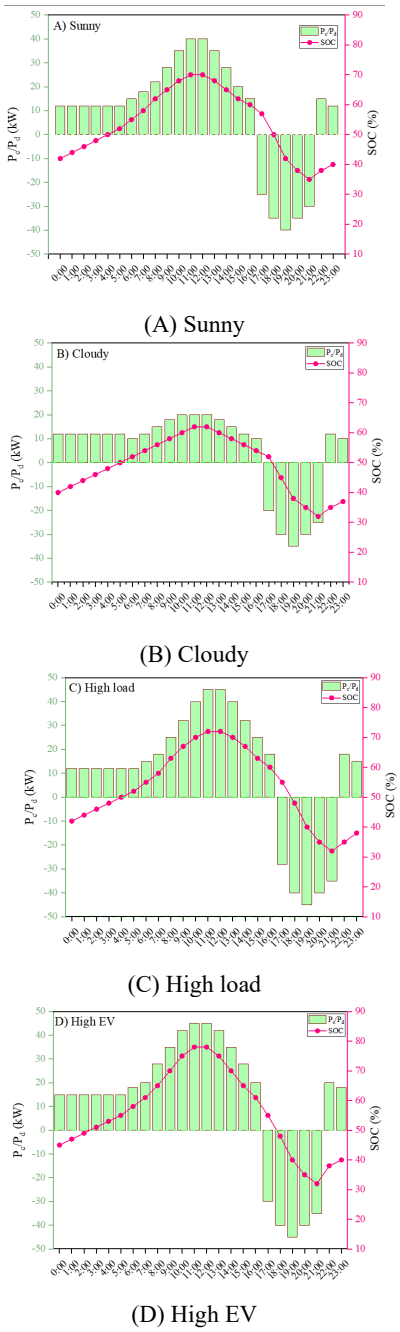

(A) Sunny

(B) Cloudy

(C) High load

(D) High EV

Figure 2. Simulated 24-hour VES Charging/Discharging Power and SOC under Four Scenarios

During the nighttime valley period (22:00–6:00), when electricity prices are low, VES recharges moderately to

restore SOC for the next day. Simulation results show that in Scenario A, the typical nighttime charging power is 10-15 kW, enabling SOC to recover from 30-35% to about 40%, ensuring sufficient capacity for absorbing surplus PV energy the following midday. In Scenario D, due to higher EV charging demand, the nighttime valley charging power slightly increases to 15–20 kW, meeting the dual requirements of EV charging and PV integration.

Overall, the SOC trajectory of VES throughout the day follows a dynamic pattern of "rising at midday, declining in the evening, and replenishing at night." This operational strategy not only enhances PV self-consumption but also significantly reduces grid purchase costs during peak hours. The degree of reliance on VES varies across scenarios: in Scenario B, dependence on its discharging capability is greater; in Scenario C, discharging demand reaches the highest level; while in Scenario D, a trade-off must be made between nighttime replenishment and midday PV absorption. In summary, VES demonstrates flexible dispatch capabilities across all typical scenarios, serving as a key enabler for PV–storage coordination, improving system economy, and enhancing operational reliability.

4.3. System Operation Performance Evaluation

After the introduction of VES and the implementation of optimal scheduling, the system performance shows significant improvement compared to the baseline scenario without energy storage. The improvements are mainly reflected in three aspects: reduction of peak-to-valley difference, improvement of PV utilization rate, and reduction of system electricity purchase costs.

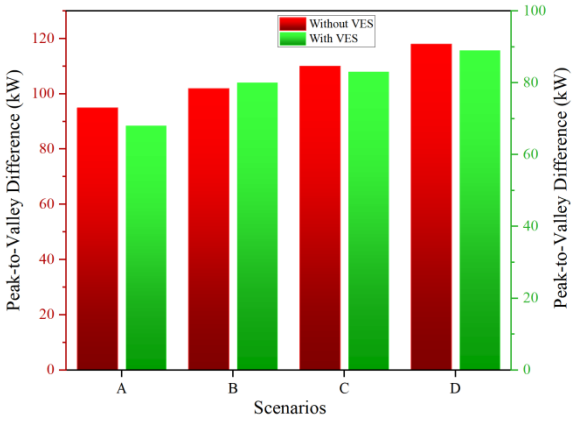

Figure 3. Peak-to-Valley Difference of Load with and without VES in the Four Scenarios

First, regarding peak shaving and valley filling, the intra-day charging and discharging behavior of VES effectively smooths the load curve. In Scenario A (sunny day), the peak-to-valley difference decreases from 95 kW in the baseline to 68 kW, achieving a peak reduction rate of 28.4%. In Scenario B (cloudy day), despite insufficient PV output, VES still reduces the evening peak load by about 22 kW, lowering the peak-to-valley difference by 21.6%. Under Scenario C (high load), the discharge capability of VES significantly reduces the maximum peak load from 144 kW to 128 kW, alleviating grid stress under high-load conditions. In Scenario D (high EV penetration), VES charges during nighttime valleys and releases approximately 38 kWh in the evening, reducing the peak-to-valley difference by 24.1% and maintaining load curve stability (see Fig. 3).

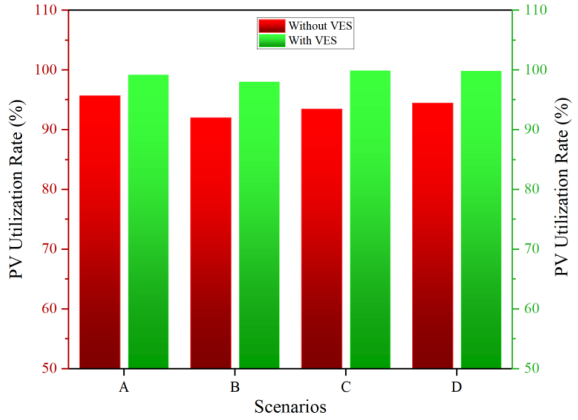

Figure 4. PV Utilization Rate with and without VES in the Four Scenarios

Second, regarding PV utilization, the VES charging strategy significantly reduces midday PV curtailment. Simulation results show that in Scenario A, PV curtailment decreases from 4.3% to 0.8%, increasing utilization to 99.2%. In Scenario B, although PV output is only 35% of that on a sunny day, VES raises the utilization rate from 92% to 98%. In Scenario C, VES absorbs 32 kWh of midday surplus PV energy, improving utilization by 6.4%. In Scenario D, due to the nighttime EV load providing additional scheduling flexibility, the coordination of midday charging and nighttime replenishment allows PV generation to be almost fully utilized (see Fig. 4).

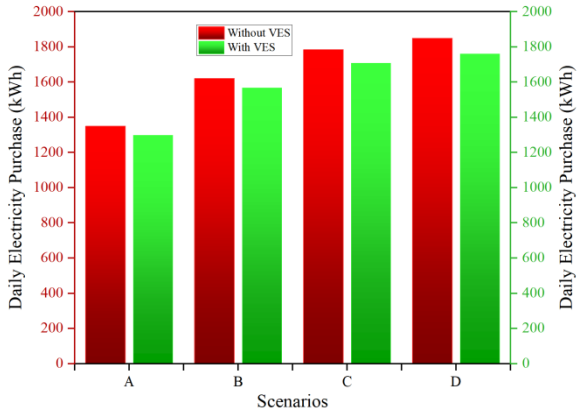

Figure 5. Daily Electricity Purchase Changes with and without VES in the Four Scenarios

Finally, regarding electricity purchase and operational costs, VES reduces overall electricity expenditure through a "valley purchase - peak reduction" strategy. Comparisons show that in Scenario A, total electricity purchase decreases from 1,350 kWh to 1,298 kWh, reducing operational costs by about 6.1%. In Scenario B, purchase costs decrease by 4.8%. In Scenario C, electricity purchases are reduced by 78 kWh, saving approximately 7.3% in costs. In Scenario D, while meeting EV charging requirements, VES reduces electricity costs by 5.5%. These results indicate that VES not only enhances renewable energy utilization but also significantly improves system economics (see Fig. 5).

4.4. Discussion and Outlook

This study constructs a multi-scenario optimization model for customer-side VES systems and systematically analyzes their role in peak shaving and valley filling, PV utilization, and electricity cost reduction. Simulation results indicate that VES can achieve flexible scheduling across different typical day scenarios, significantly enhancing both the economic efficiency and operational stability of the system, while also verifying the feasibility and effectiveness of coordinated scheduling among multiple types of customer-side resources.

In the typical sunny-day scenario, VES charges during the midday PV generation peak and discharges during the evening load peak, effectively reducing the peak-to-valley difference and improving local PV consumption. This scheduling strategy not only improves the match between user-side load and PV output but also mitigates grid load fluctuations by leveraging storage flexibility. Consistent with previous studies, distributed energy storage under flexible scheduling can significantly alleviate the impact of renewable energy variability on the grid [23]. Simulation results show that VES absorbs excess PV energy at noon and discharges in the evening, achieving notable peak shaving while reducing reliance on grid electricity during peak hours, thereby improving overall system economic performance.

Under cloudy or low-irradiance conditions, despite limited PV output, VES can still regulate charging and discharging to smooth the load and reduce electricity purchases. This demonstrates that customer-side virtual energy storage possesses certain flexibility and robustness under uncertainty, helping the system adapt to external uncertain events [24]. Particularly under high-load scenarios, VES can discharge energy to reduce evening peak loads, alleviating grid dispatch pressure, reducing high-cost electricity purchases, and improving system stability.

From an economic perspective, optimized VES scheduling significantly lowers electricity costs while increasing PV self-consumption and the utilization efficiency of customer-side resources. This indicates that virtual energy storage not only provides technical peak-shaving and valley-filling functions but also enhances proactive demand-side participation under market-based mechanisms [25]. In scenarios with high EV penetration, VES scheduling can accommodate both EV charging demand and PV absorption, achieving effective peak-valley load balancing and demonstrating the advantage of virtual storage in coordinating multiple resource types.

However, this study has certain limitations. First, the simulation scenarios and data are relatively idealized and do not fully cover seasonal weather variations, load randomness, or extreme fluctuations in PV output, which may underestimate operational uncertainties. Second, the optimization objectives mainly focus on economic performance and PV utilization, without fully considering storage degradation, user comfort, or the effects of more complex electricity market mechanisms on scheduling strategies [26]. Previous studies have shown that storage degradation can significantly affect long-term operational performance; therefore, future research could incorporate storage lifetime degradation models and uncertainties in electricity price forecasts to enhance the practical applicability and decision-making value of the model [27].

Overall, customer-side VES demonstrates significant potential to enhance grid flexibility, promote renewable energy consumption, and optimize system economics, but its performance is highly dependent on weather conditions, load characteristics, and market environment. Future research should integrate larger-scale measured data, consider storage degradation and user behavior models, and incorporate more complete market mechanisms to further optimize coordinated scheduling strategies for multiple types of customer-side resources, thereby promoting the practical deployment of VES in real-world power systems [28].

5. Conclusions

This paper proposes an integrated framework for the identification and optimal scheduling of VES using multiple types of customer-side resources. By establishing quantitative models for thermostatically controlled loads, electric vehicles, and distributed energy storage systems, the framework effectively captures key VES characteristics such as equivalent capacity, charging/discharging power, self-discharge rate, and user comfort. A data-driven clustering method is employed to aggregate heterogeneous resources, and an optimal scheduling model is developed to minimize the total operational cost of the aggregator.

Simulations under four typical scenarios-sunny, cloudy, high load, and high electric vehicle penetration-demonstrate that the proposed VES scheduling strategy effectively enables a typical operational mode of "midday charging-evening discharging-nighttime replenishment," significantly improving system performance. The results show that the peak-to-valley difference is reduced by 21.6% - 28.4%, the photovoltaic utilization rate is increased to over 98%, and electricity purchase costs are decreased by 4.8% - 7.3%. These findings confirm the

notable effectiveness of VES in enhancing both economic efficiency and operational reliability of the system.

The integrated framework and optimization method proposed in this study provide an effective technical pathway and solution for coordinating multiple types of customer-side resources, promoting the integration of renewable energy, and supporting the sustainable operation of power systems.

Acknowledgments.

This work was financially supported by the Research and Application of a "One-Stop" Virtual Energy Storage New Model and Business Paradigm Based on Cloud Collaboration (5211LS240003).

References

[1] Jafarizadeh H, Yamini E, Zolfaghari SM, Esmaeilion F, Assad MH, Soltani M. Navigating challenges in large-scale renewable energy storage: Barriers, solutions, and innovations. Energy Rep. 2024; 12: 2179-2192.

[2] Mariam S, Boudet E, Ferrier B, Perrin A, Petit M. Loads scheduling for demand response in energy communities. Comput Oper Res. 2023; 160: 106358.

[3] Fonseca T, Ferreira LL, Landeck J, Klein L, Sousa P, Ahmed F. Flexible loads scheduling algorithms for renewable energy communities. Energies. 2022; 15: 8875.

[4] Kamana-Williams B, Bishop D. Flexible futures: The potential for electrical energy demand response in New Zealand. Energy Policy. 2024; 195: 114387.

[5] Sawilam M, Kizilkaya B, Taha A, Flynn D, Imran MA, Ansari S. Impact of virtual power plants on grid stability and renewable energy integration in smart cities using IoT. Energy Rep. 2025; 13: 3312-3323.

[6] Niu J, Tian Z, Zhu J, Yue L. Implementation of a price-driven demand response in a distributed energy system with multi-energy flexibility measures. Energy Convers Manag. 2020; 208: 112575.

[7] Abdelkader S, Amissah J, Abdel-Rahim O. Virtual power plants: An in-depth analysis of their advancements and importance as crucial players in modern power systems. Energy Sustain Soc. 2024; 14: 52.

[8] Nowbandegani MT, Nazar MS, Javadi MS, Catalao JP. Demand response program integrated with self-healing virtual microgrids for enhancing the distribution system resiliency. Int J Electr Power Energy Syst. 2024; 157: 109898.

[9] Li Y, Li K, Yang Z, Yu Y, Xu R, Yang M. Stochastic optimal scheduling of demand response-enabled microgrids with renewable generations: An analytical-heuristic approach. J Clean Prod. 2022; 330: 129840.

[10] Han C, Witthaut D, Rydin GL, Bottcher PC. Collective effects and synchronization of demand in real-time demand response. J Phys Complex. 2022; 3: 025002.

[11] Amini M, Almassalkhi M. Optimal corrective dispatch of uncertain virtual energy storage systems. IEEE Trans Smart Grid. 2020; 11(5): 4155-4166.

[12] Sivaneasan B, Kandasamy NK, Lim ML, Goh KP. A new demand response algorithm for solar PV intermittency management. Appl Energy. 2018; 218: 36-45.

[13] Muessel J, Ruhnau O, Madlener R. Accurate and scalable representation of electric vehicles in energy system models: A virtual storage-based aggregation approach. iScience. 2023; 26: 107816.

[14] Jin B, Liu Z. Evaluating the impact of virtual energy storage under air conditioning and building coupling on the performance of a grid-connected distributed energy system. J Build Eng. 2024; 89: 109309.

[15] Fu Q, Xing Z, Zhang C, Xu J. A review and prospective study on modeling approaches and applications of virtual energy storage in integrated electric–thermal energy systems. Energies. 2024; 17: 4099.

[16] Xie K, Hui H, Ding Y. Review of modeling and control strategy of thermostatically controlled loads for virtual energy storage system. Prot Control Mod Power Syst. 2019; 4: 23.

[17] Conte F, Vergagni MC, Massucco S, Silvestro F, Ciapessoni E, Cirio D. Performance analysis of frequency regulation services provided by aggregates of domestic thermostatically controlled loads. Int J Electr Power Energy Syst. 2021; 131: 107050.

[18] Zhou B, Jiang Y, Zhang Y, Li G, Gu P, Liu B. Review of modelling and optimal control strategy for virtual energy storage. IET Gener Transm Distrib. 2025; 19: 70031.

[19] Jiang Y, Zhou B, Li G, Luo Y, Hu B, Liu Y. Virtual energy storage-based charging and discharging strategy for electric vehicle clusters. World Electr Veh J. 2024;15:359.

[20] Li Y, Wang K, Xu C, Wu Y, Li L, Zheng Y, Yang S, Wang H, Ouyang M. The potentials of vehicle-grid integration on peak shaving of a community considering random behavior of aggregated vehicles. Next Energy. 2025; 7: 100233.

[21] García-Miguel PLC, Alonso-Martínez J, Arnaltes Gómez S, García Plaza M, Asensio AP. A review on the degradation implementation for the operation of battery energy storage systems. Batteries. 2022; 8: 110.

[22] Brouyaux L, Iacovella S, Quoilin S. A Real-Life Demonstration of Secondary Frequency Reserve Provision with Electric Water Heaters. Energies. 2025; 18(7): 1704.

[23] Burgio A, Cimmino D, Dolatabadi M, Jasinski M, Leonowicz Z, Siano P. Virtual energy storage system for peak shaving and power balancing the generation of a MW photovoltaic plant. Energy Storage. 2023; 71: 108204.

[24] Koirala BP, Oost E, Windt H. Community energy storage: A responsible innovation towards a sustainable energy system. Appl Energy. 2018; 231: 570-585.

[25] [25] Cao W, Yu J, Xu M. Optimization scheduling of virtual power plants considering source-load coordinated operation and wind–solar uncertainty. Processes. 2024; 12: 11.

[26] Ruan G, Qiu D, Sivaranjani S, Awad AS, Strbac G. Data-driven energy management of virtual power plants: A review. Adv Appl Energy. 2024; 14: 100170.

[27] Liu X, Niu Z, Li Y, Hu L, Tang J, Cai Y, Zeng S. Optimal demand response for a virtual power plant with a hierarchical operation framework. Sustain Energy Grids Netw. 2024; 39: 101443.

[28] Burgio A, Cimmino D, Dolatabadi M, Jasinski M, Leonowicz Z, Siano P. Virtual energy storage system for peak shaving and power balancing the generation of a MW photovoltaic plant. Energy Storage. 2023; 71: 108204.